TRANSACTIONS ON ELECTROMAGNETIC SPECTRUM

A High-Gain Reflector- DGS-Superstates -Enabled Quad-Band 5G-Antenna for mm-wave Applications

Aafreen Khan [1] *, Anwar Ahmad [1], Maksud Alam [2]
[1]Department of Electronics and Communication Engineering, Jamia Millia Islamia, New Delhi, India
[2]Department of Computer Science and Engineering, Galgotia College of Engineering and Technology, Greater Noida, India
Email: aafreen.khan1994@gmail.com, aahmad4@jmi.ac.in, alam.maksud@gmail.com

*** Corresponding author's e-mail address:** aafreen.khan1994@gmail.com

Received: 8 August 2023
Revised: 15 September 2023
Accepted: 20 September 2023

Research Article
Vol. 3 / No. 1 / 2024
Doi: 10.5281/zenodo.8363039

Abstract: The mm-wave antenna, consisting of a reflector, a DGS structure, and two superstates using Taconic (CER-10) and silicon, has been presented in this article. In the proposed antenna, a DGS with a reflector and two superstates is implemented to improve the antenna performance characteristics. The designed configuration (ANT-S5) is resonating on four mm-wave bands m1=41.7241GHz (41.1102-42.347) GHz, m2=48.9655GHz (48.637-49.1061) GHz, m3=63.2414GHz (61.142-66.137) GHz, m4=76.069GHz (73.4655-78.859) GHz and the maximum achieved gain is 12.02dBi at the 41.3103GHz along with the AR<3dB bands (76.1777-77.2794) GHz, (69.662-70.509) GHz. The designed antenna has been simulated on HFSS software and is convenient for 5G mm-wave applications.

Keywords: Quad Band, Gain, DGS, mm-wave

Cite this paper as: Khan A, Ahmad A, Alam M. A High-Gain Reflector- DGS-Superstates -Enabled Quad-Band 5G-Antenna for mm-wave Applications. Transactions on Electromagnetic Spectrum. 2024; 3(1): 34-50, Doi: 10.5281/zenodo.8363039

1. INTRODUCTION

The antenna is an important element in wireless communication. Various types of antennas are available. Microstrip patch antennas are important because of their lightweight, compact size and simple structure design. Increasing attention towards the 5th generation due to advantageous features of 5G like high data rate and low latency, but the disadvantage of absorption due to the atmosphere at the high frequency has drawn the attention of antenna designers to design an antenna with high gain characteristics. To achieve high gain, various methods like antenna arrays can be implemented, but it makes the structure bulky and complex. So, in the proposed structure design, the reflector surface and superstates have been implemented along with the DGS, and the large value of the gain has been achieved.

In [1-5], the 5G antennas with DGS structure have been designed. Also, DGS structure is used to improve the performance parameter of the antenna such as in arc shape DGS antenna, the cross-polarization has been

suppressed by using the DGS structure [6]. A patch antenna with cross-polarization has been improved using a non-proximal symmetric DGS structure [7]. The higher-order harmonics have been suppressed by using the DGS structure in [8]. Cross polarization has been reduced by using resonant-type DGS [9]. In the microstrip array, radiation property has been improved with integrated DGS [10]. The concrete ring-shaped DGS has been implemented in [11] to suppress the leakage. In [12], to get the circular patch with improved radiation, asymmetric and compact DGS configuration has been used. In an S-shaped antenna, high isolation has been obtained by using DGS structures [13]. In [14], the cross-polarization has been reduced by using the asymmetric geometry of DGS. Monopole antenna [15] uses the DGS structure for enhancement of bandwidth. An antenna array is the most useful to achieve better antenna characteristics, for instance in [16-18], the 2×2 array has been used, and a good gain is achieved. In a steerable antenna, four elements form an array, and a good peak gain of 8.4 dBi and 11.7 dBi has been achieved [19]. However, the disadvantage is that it makes the antenna bulky and complex in structure. So instead of using an array, another method like reflector surfaces and the superstates can be used to enhance the gain and to get good antenna parameters. Also, in [20], the antenna is a single band resonating with the DGS structure, and the gain is less. While the [21] also single band resonating with the metamaterial implementation and the gain achieved is less as compared to the proposed structure, and in all-textile PIFA [22], the antenna is single band resonating. The gain achieved is also less as compared to the proposed antenna structure with the DGS. The reflector and two superstates' methods have been implemented, and a high gain has been achieved for the mm-wave applications.

2. ANTENNA STRUCTURE DESIGN

The antenna structure has been designed using RT-duroide material ε_r=2.2 substrate on the ground plane of area 4.325×4.976 mm^2, and the rectangular patch of area 1.5×1.976 mm^2 is mounted on the substrate of height h_1=0.5mm. A rectangular patch has been designed, which is shown in Figure 1(b). The ground structure has been modified; the modified ground plane is given in Figure 1(c). Modification in the ground plane has been done by cutting the L, T and circular shape slots on the ground. These slots are changing the antenna performance characteristics further for improvement in gain parameters. The reflector surface with the size of 6mm×6mm has been added. The addition of the reflector surface, which has been given with dimensions in Figure 1(d), focuses energy in one direction or increases the directivity and gain. For further enhancement of gain, the superstate has been implemented. In the proposed antenna structure, the two superstates have been implemented, named superstate 1 and superstate 2, which is given in Figure 1(e) with the permittivity of ε_{r2}=11.9 and ε_{r3}= 10 with the height of h_2=0.4mm and h_3=0.25mm the superstates implementation is done, one by one and the evolution of the proposed antenna (ANT-S5) is given in Figure 2 through 2(a),2(b),2(c),2(d),2(e) intermediate designs. Both superstate implementations are increasing the gain, and the designed antenna resonates on the mm-wave and is a useful one for 5G mm-wave applications. The antenna is simulated on the HFSS software, and the proposed antenna specifications are shown in Table 1.

Table 1. Proposed Antenna Specifications

Antenna dimension	Specification(mm)	Antenna dimension	Specification(mm)
L=Ls1=Ls2	4.325	b2	3.05
W=WS1=WS2	4.976	b3	3.2
L1	1.325	t1	0.3
W1	1.976	t2	0.4
h1	0.5	t3	0.5
h2	0.4	t4	0.45
h3	0.25	t5=t6	0.2
s1	0.5	g1	1.4
s2	3	g2	1.6
s3	1.1	g3	1
b1	4.7	Ls3=WS3	6

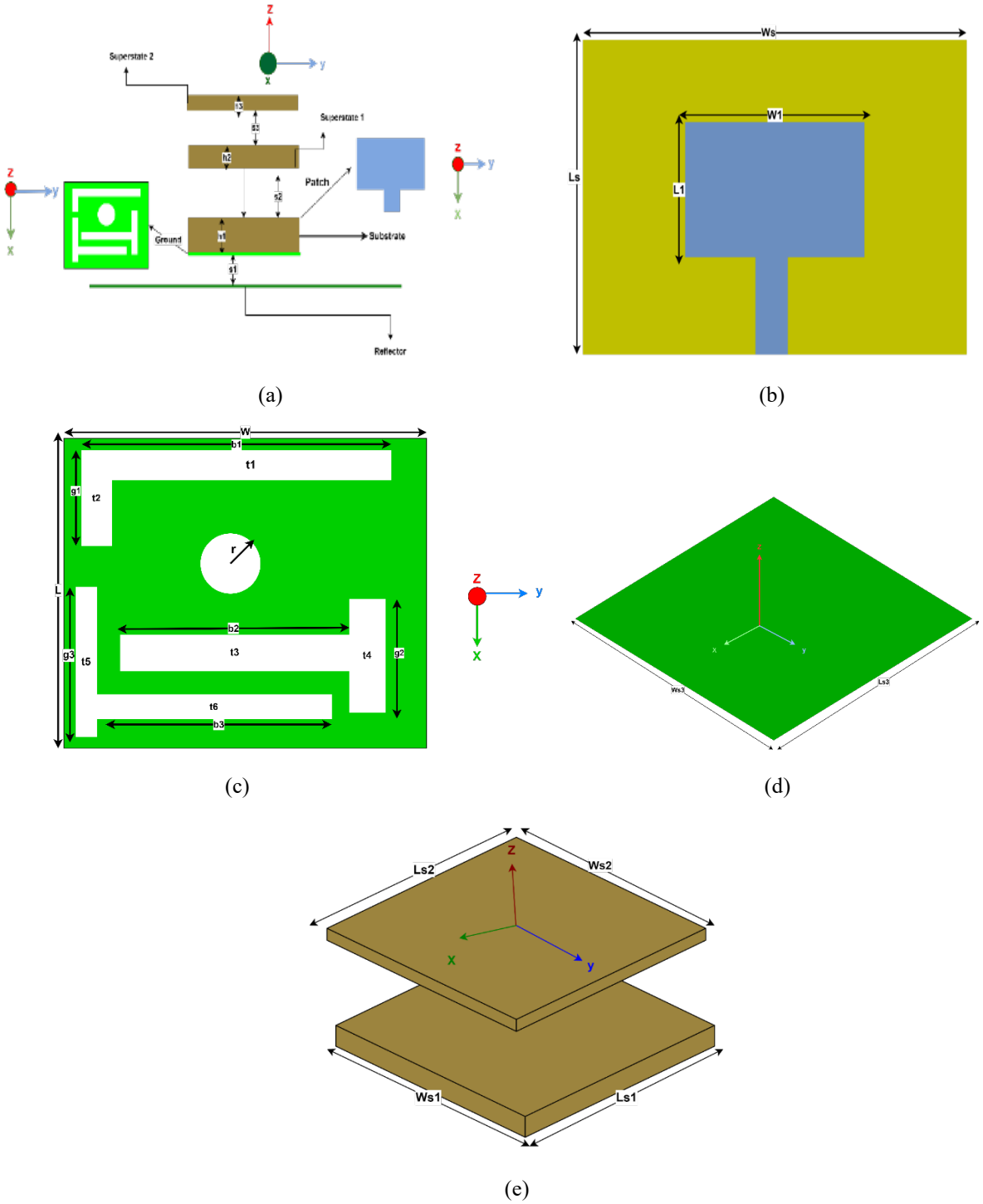

Figure 1. (a) 3D orientation of proposed superstates (b) Proposed ANT -S5 front orientation (c) Proposed DGS structure (d) Front view of the Rectangle Patch (e) Proposed Reflector Structure

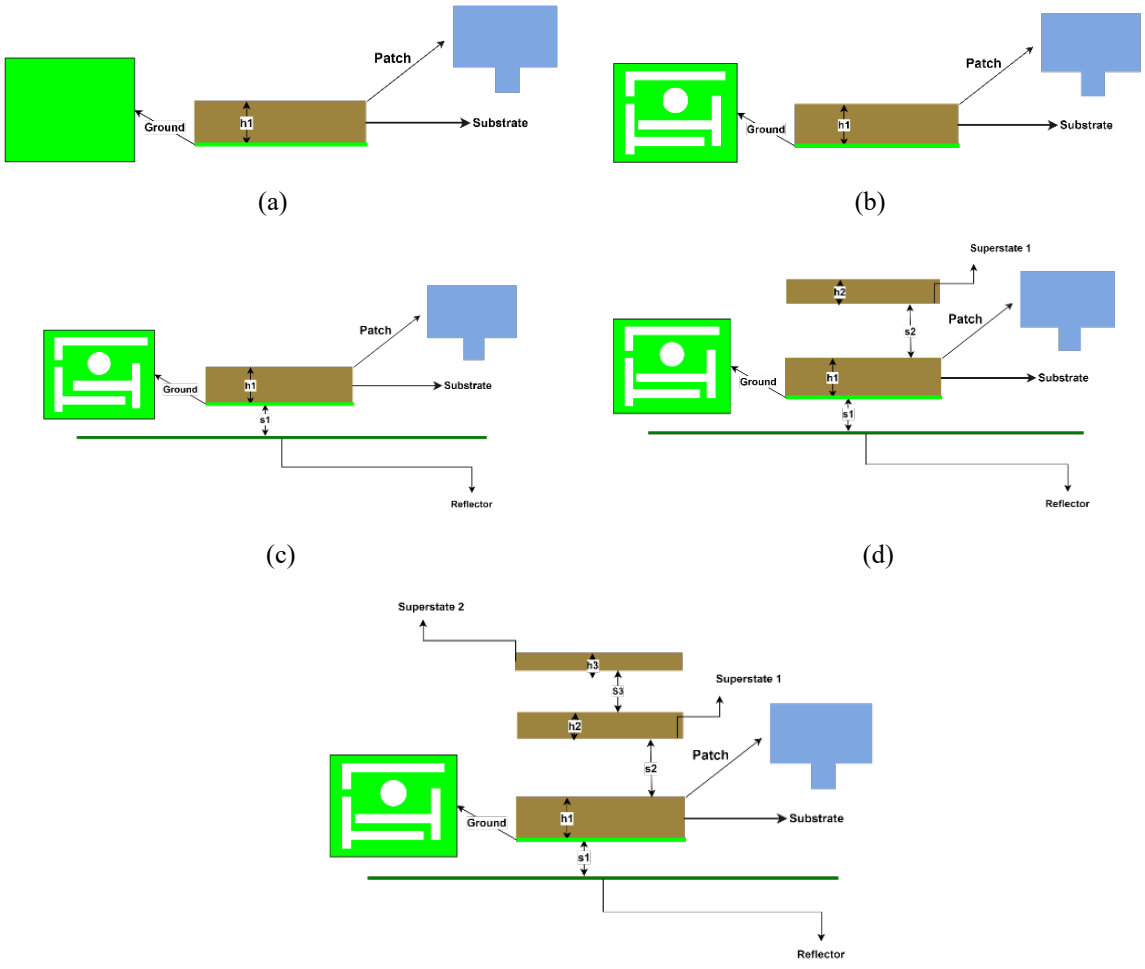

Figure 2. (a) Plain Ground structure (b) with DGS (c) With DGS and Reflector (d) with DGS Reflector and Superstate (e) with DGS reflector and double Superstates.

Rectangle patch antenna without any technique application consists of one resonating frequency m1=70.2759GHz (66.7304-73.5986) GHz with the return loss parameter of -20.869dB and the gain value 8.3987dBi, achieved at the frequency 80 GHz. The characteristics of the designed antenna with the other techniques implementation are given in Figure 5(a),(b),(c).

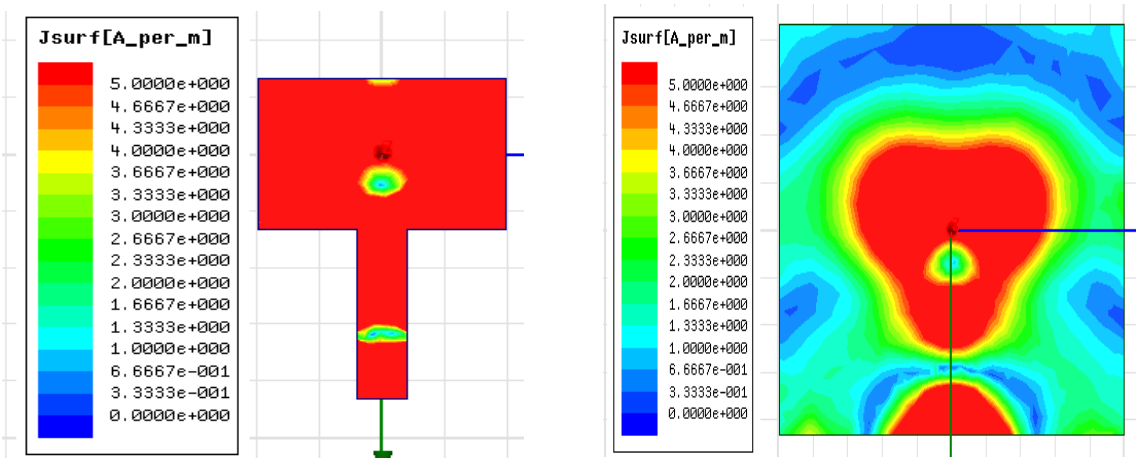

Figure 3. (a) Patch current distribution Plot (b) Ground Current distribution plot at 70.275GHz frequency

Also, the current distribution plot is given in Figure 3(a) and (b) for the patch and ground plane at the resonating frequency of 70.275 GHz.

3. RESULT ANALYSIS AND DISCUSSION

3.1 Distorted Ground plane (DGS) (step-1)

Distorted ground structure (DGS) is a helpful technique to improve antenna performance parameters in [1-10]. The DGS structure has been used to improve the antenna characteristics of the proposed antenna structure, the DGS structure has been implemented in the designed antenna, and the evolution of the DGS structure has been represented in Figure 4 (a),(b),(c),(d).

In step 1, the DGS structure, the GS1, GS2, GS3, and GS4 slots have been etched out from the ground plane. With the evolution of the DGS structure, the various characteristics of the antenna have been represented in Figure 5 (a), (b), (c), and (d). In the evolution of the DGS structure, the GS1 shape slot has been etched out which is given in Figure 3(a). After etching of the GS1 from the ground, the antenna is resonating on the three frequency bands, these bands are m1=28.4828 GHz (28.1599-28.9636) GHz, m2=45.6552GHz (44.67846.6424) GHz, m3=60.7586 GHz (59.1983-78.1706) GHz with the return loss parameter -22.0344dB, -15.3816dB, -22.5799dB respectively and the gain value obtained is 7.0883dBi at the resonating frequency 38.2069GHz. These resonating bands and gain values are given in Figure 5(a). So, slot GS1 in the ground plane is creating two more resonances along with a decrease in the maximum gain value.

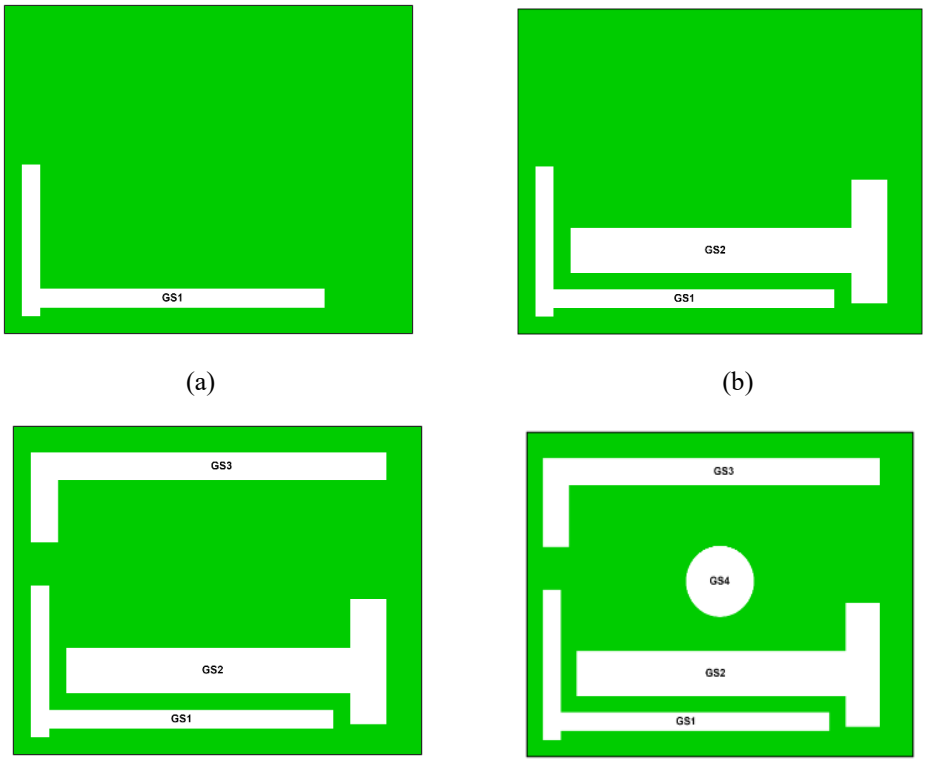

Figure 4. Evolution of proposed Antenna Ground Plane (a) Slot GS1 (b) Slot GS1+GS2 (c) slot GS1+GS2+GS3 (d) Slot GS1+GS2+GS3+GS4

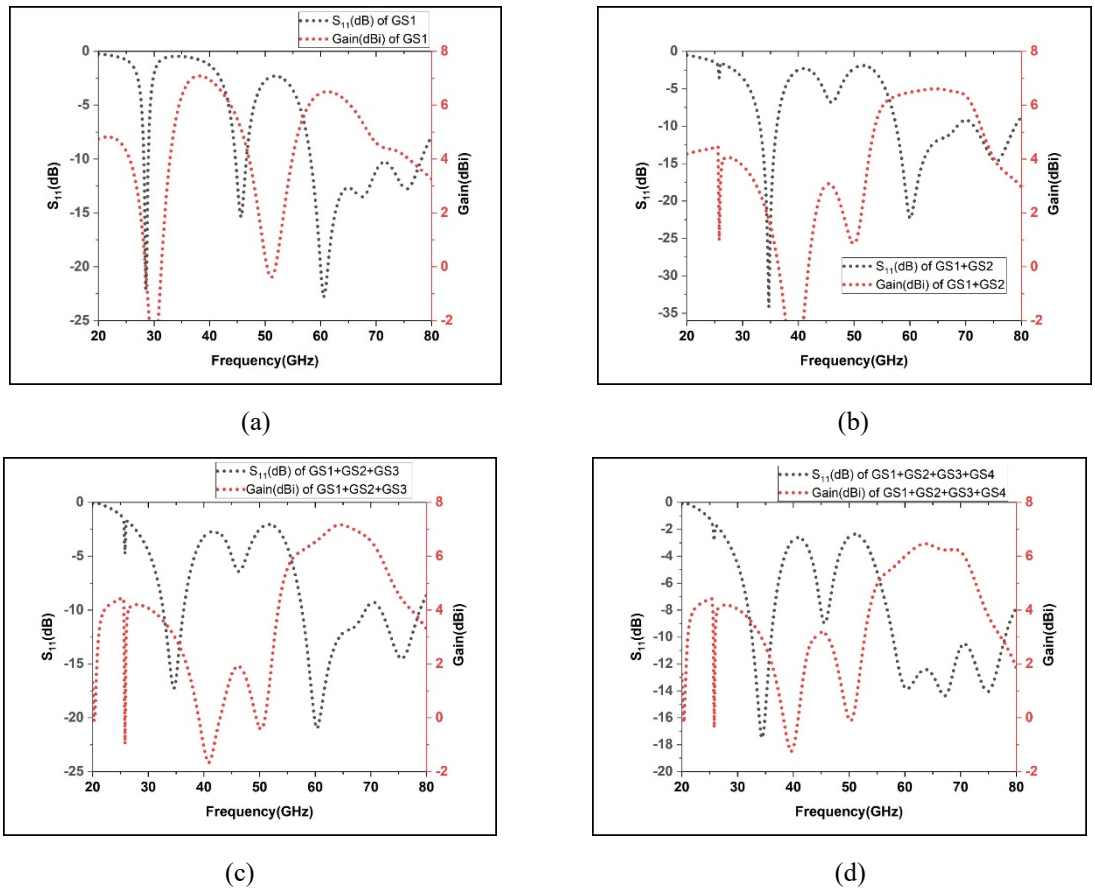

Figure 5. Return Loss and Gain V/s Frequency plots (a) For GS1 (b) GS1+GS2 (c) GS1+GS2+GS3 (d) GS1+GS2+GS3+GS4

Further in the evolution of DGS, the GS1 and GS2 have been etched out, which is given in Figure 3(b). Now the antenna is again resonating on three frequency bands these bands are m1=34.689 GHz (33.104-36.1334) GHz, m2=60.1379 GHz (57.5306-68.4927) GHz, m3=75.6552 (71.51564-78.9184) GHz with the RL values -34.1731dB, -22.351dB, -14.6569 dB respectively. And the maximum gain frequency is 64.4828 GHz with a value of 6.6109dBi. Etching of GS2 along with GS1 shifts the resonances on the higher side, and more widened bands are achieved at the cost of a decrease in the maximum gain value, which is shown in Figure 5(b). Now, the GS1+GS2+GS3 slot structures have been etched out, which is shown in Figure 4(c). In this case, also the three resonating frequency bands have been achieved these bands are m1=34.6897GHz (32.6800-36.348) GHz, m2=60.3448 GHz (57.618-69.011) GHz, m3=75.862GHz (71.778-78.810) GHz and the RL values are the -17.221dB, -20.983GHz, -14.417dB respectively. And the maximum gain value is 7.1693dBi at the frequency 64.482 GHz. The frequency and gain plots have been represented in Figure 5(c). The slot GS3 is slightly affecting the resonance frequencies. It is participating again in enhancing the gain parameter. Lastly, one more slot in the ground plane shown in Figure 4(d) has been introduced called GS4 (Circular shape). In this case, only two resonating bands are present, which are m1=34.482GHz (32.574-36.039) GHz, m2=67.1724GHz (57.848-77.9844) GHz, and RL corresponds to these frequencies are -17.4836dB, -14.370dB respectively. And the maximum gain is 6.4614 dBi at 63.6552GHz given in Figure 5(d). The GS4 slot combines the two higher resonating frequency bands, and the single wide band is achieved at a higher frequency. As the bandwidth is increasing, this is reducing the maximum gain value.

3.2 Reflector+ DGS (step-2)

In the next step 2, the reflector of a rectangle shape has been added. The dimensions of the rectangle reflector are 6mm ×6 mm. When the Reflector Surface technique is used the antenna is resonating on four resonating

bands; these bands are m1=26.827GHz (26.1772-27.256) GHz, m2=41.9310GHz (41.0555-42.754) GHz, m3=62.620GHz (58.572-67.218) GHz, m4=76.069GHz (70.668-79.329) GHz and the return loss has been observed at these frequency bands are -15.968dB, -16.183dB, -15.145dB, -23.835dB and the maximum gain value obtained is 9.430dBi at 42.137GHz. The values of resonating frequency and gain can be seen in Figures 7(a) and (b). The parameter called axial ratio is also the point of interest to observe the circular polarization property of the antenna, so when the reflector surface is added, the AR<3 dB bandwidth frequency ranges are (69.3577-73.527) GHz, (51.917-52.3600) GHz, (45.339-45.662) GHz. Also, the plot between the axial ratio and frequency with Reflector and DGS has been represented in the comparative Figure 7(c). The current distribution plot of the proposed DGS structure has been represented in Figures 6 (a) and (b). The intense current distribution that has been represented by red colour is shown in the plot near the L and GS1, GS2, GS4 slots, and these slots are creating the multi-resonant characteristics in the proposed antenna structure.

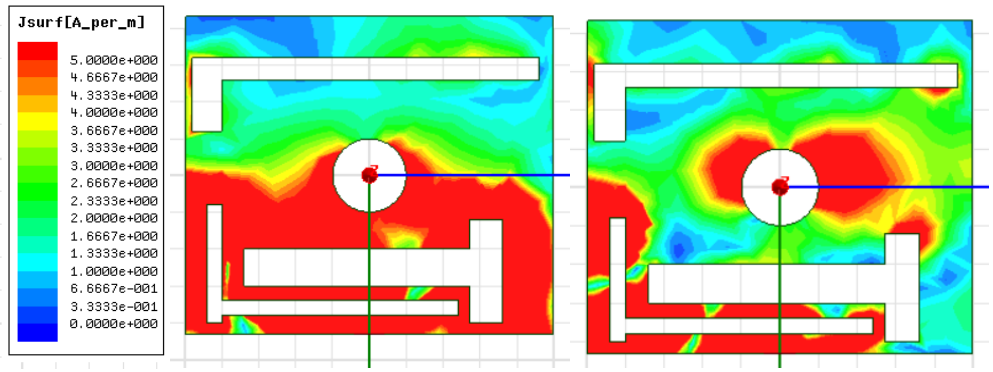

(a) (b)

Figure 6. Current distribution plot (a) at 34.482GHz (b) at 67.172GHz

Table 2. Parameters value with DGS structure

DGS Structure	Resonating frequency bands (GHz)	Bandwidth (GHz)	Return Loss (dB)	Maximum Gain (dBi)
GS1	(28.1599-28.9636) (44.678-46.6424) (59.1983-78.1706)	0.80 2 18	-22.0344 -15.3816 -22.5799	7.0883
GS1+GS2	(33.104-36.1334) (57.5306-68.4927) (71.51564-78.9184)	3.02 10.962 7.403	-34.1731 -22.351 -14.6569	6.6109
GS1+GS2+GS3	(32.6800-36.348) (57.618-69.011) (71.778-78.810)	3.668 11.393 7.032	-17.221 -20.983 -14.417	7.1693
GS1+GS2+GS3+GS4	(32.574-36.039) (57.848-77.9844)	3.465 20	-17.4836 -14.370	6.4614

To understand the slot effects in the ground plane, we can also analyze the impact of the single slot on the parameter of the antenna.

3.3 Reflector +DGS+ Superstate 1 (step-3)

In step-3, the superstate of dimensions 4.325mm×4.976mm and permittivity 11.9 has been applied. This implementation changes the antenna characteristics; after this implementation, the antenna resonates on three frequency bands; these bands are m1=41.3103GHz(40.711-41.921)GHz, m2=63.034(60.818-65.994)GHz, m3=76.275GHz(72.578-78.869) GHz and the return loss corresponds to these frequencies are -16.078dB,

-32.5110dB, -19.803dB respectively and the maximum gain in this step is 11.1958dBi, also the axial ratio band achieved is one in this case which covers the frequency range (43.1332-43.2330)GHz. So these parameters are also represented in Figure 7 (a), (b) and (c).

3.4 Reflector +DGS+Superstate1+Superstate 2 (step-4)

In step-5, another superstate of dimensions 4.325mm×4.976mm and permittivity with 10 has been added. In this case, the resonating bands achieved are four with the values m1=41.724GHz (41.1102-42.347) GHz, m2=48.9655GHz (48.637-49.1061) GHz, m3=63.2414GHz (61.142-66.137) GHz, m4=76.069GHz (73.4655-78.859) GHz and the RL value achieved at these frequency bands are -18.017dB, -10.727dB, -29.042dB, -16.6700dB respectively. The maximum gain was achieved at 41.3103GHz and the value is 12.0216dBi. The AR<3dB bands are (76.1777-77.2794) GHz, and (69.662-70.509) GHz. So, the comparative analysis of all the parameters has been represented in Figure 7(a), (b) and (c). Also, in Table 3, the performance parameter has been represented.

Table 3. Performance Parameter of the antenna with the implementation of Different Techniques

Techniques	Centre Frequency (GHz)	Resonating Frequency Bands	Return Loss (dB)	Maximum Gain (dBi)	Axial Ratio<3dB Bands (GHz)
Rectangle patch	70.275	66.7304-73.598	-20.869	8.3987	No bands
Rectangle Patch +DGS	34.482 67.172	32.574-36.039 57.848-77.984	-17.483 -14.370	6.461	67.150-68.891 51.062-51.331
Rectangle Patch +DGS +Reflector	26.827 41.9310 62.620 76.069	26.177-27.256 41.055-42.7545 58.572-67.218 70.668-79.329	-15.968 -16.183 -15.145 -23.218	9.430	69.357-73.527 51.917-52.360 45.339-45.662
Rectangle Patch +DGS +Reflector +Superstate 1	41.310 63.034 76.275	40.7118-41.921 60.8185-65.994 72.578-78.869	-16.078 -32.511 -19.803	11.195	43.1332-43.233
Rectangle Patch +DGS +Reflector +Superstate 1 +Superstate 2	41.7241 48.965 63.241 76.069	41.110-42.347 48.637-49.106 61.142-66.137 73.465-78.859	-18.017 -10.727 -29.042 -16.670	12.021	76.1777-77.279 69.662-70.509

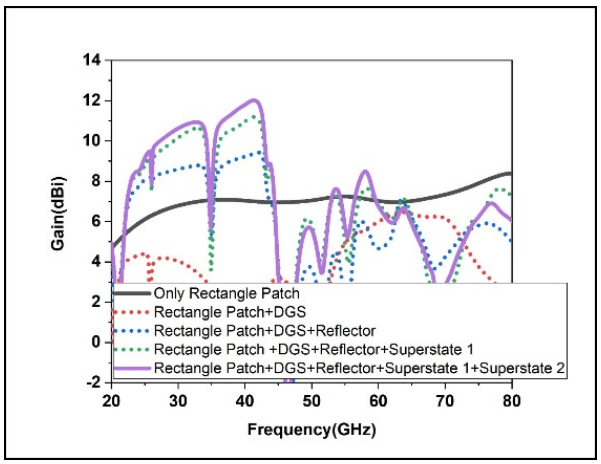

(a)

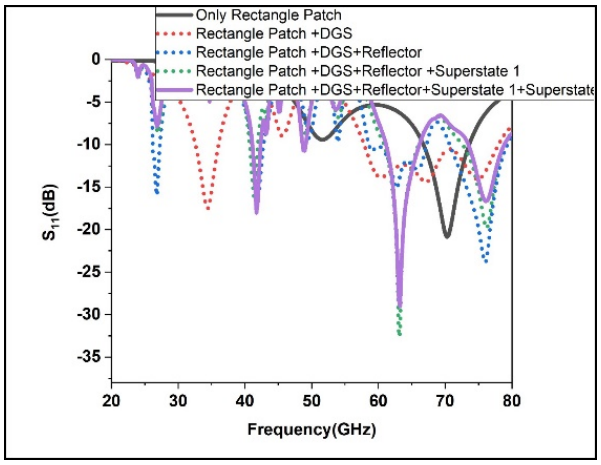

(b)

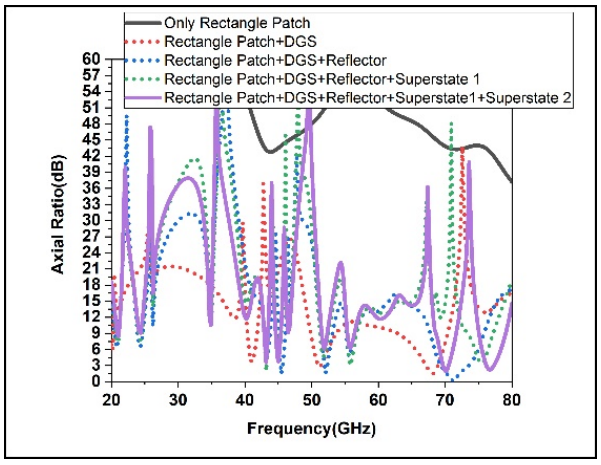

(c)

Figure 7. (a) Gain plot with different techniques (b) Return loss plot (c) Axial Ratio

The importance of the DGS structure can be realized in the proposed article by comparing the two antennas. If the whole antenna with DGS + reflector and superstate 1 +Superstate 2 are considered as ANT-S1 and the antenna without DGS+ reflector+ Superstate 1+Superstate 2 is considered as ANT-S5 then the comparative analysis has been represented in Figure 8(a), (b), (c), where the return loss, gain, and AR has been compared as these parameters are important to analyze the performance of the antenna. So, in Figure 8(a), the return loss parameter for ANT-S1 which has been represented by the solid black line in the plots. The two resonating frequencies are m1= 57.5136GHz (49.948-59.005) GHz, m2=71.5172GHz (68.6162-73.265) with the RL value -15.513dB, -32.943dB. And the maximum gain achieved is 10.8215dBi at the frequency 58. 0690GHz.

Also, for the ANT-S1, the ground plane current distribution is shown in Figure 9(a) and (b) at different resonance frequencies.

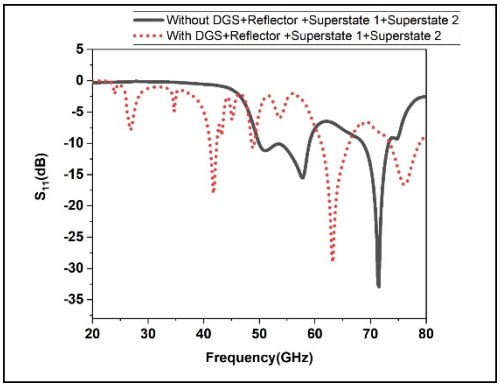

(a)

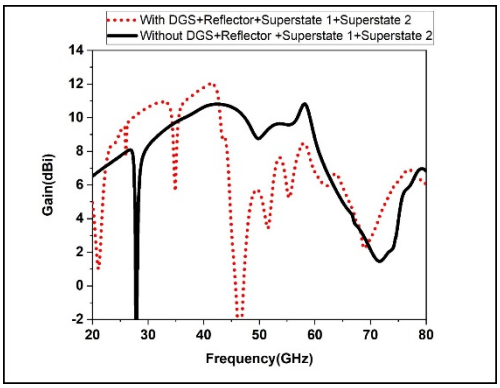

(b)

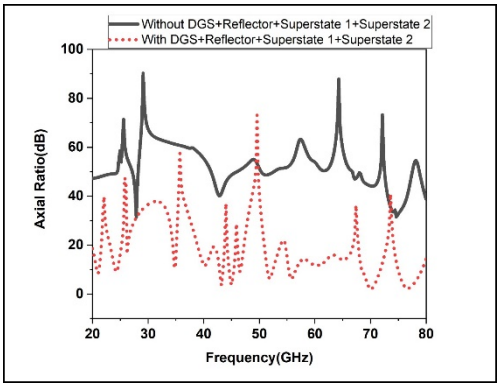

(c)

Figure 8. Comparison between ANT-S1 and ANT-S5 (a) S_{11} parameter (b) Gain Parameter (c) Axial Ratio Parameter

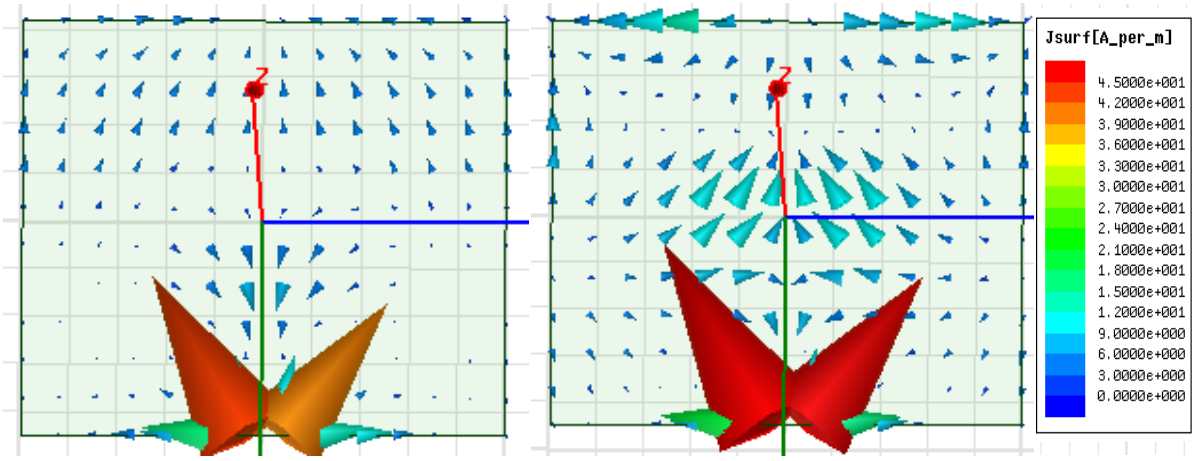

(a) (b)

Figure 9. Proposed Antenna (ANT-S1) Current Distribution (a) at 57.862GHz (b) 71.517GHz

The structure with slot GS1 in the ground plane and Reflector and both the superstate (ANT-S2) is resonating on the five bands; these bands are m1=64.8966GHz (62.582-69.179) GHz, m2=56.6207 GHz (56.3757-56.736) GHz, m3= (44.555-44.9388) GHz, m4=31.379 (31.247-31.465) GHz, m5=25.793 GHz (25.552-25.924) GHz. The return loss parameter at these frequencies are -29.6554 dB, -10.114 dB, -10.791dB, -13.518dB, -13.5355dB, respectively. These values can be seen in Figure 8(a) also, the ANT-S2 has the maximum gain at the frequency of 30.1379 GHz, and the value obtained is 10.790dBi, which has been represented in Figure 9(a-b), the axial ratio parameter is also given in Figure12(c) which represents that the circular polarization (CP) bands for ANT-S2 are (71.6248-72.4500 GHz, (32.8271-32. 8278) GHz, (21.175-21.298) GHz.

The structure called ANT-S3 has the slots GS1and GS2 in the ground plane along with the reflector and both the superstates in the ANT-S3 also, the resonating bands are five, these are m1 24.3448GHz (24.2191-24.596)GHz, m2=38.620GHz (38.235-38.944) GHz, m3=44GHz (43.683-44.351)GHz, m4=63.821GHz (59.7120-66.937)GHz, m5=76.4828GHz (75.074-77.898) GHz and the return loss achieved -11.586dB, -12.364dB, -22.909dB, -21.7933dB, -10.910dB respectively and the maximum gain is 10.975dBi at the 33.0345 GHz for ANT-S3. The axial ratio <3dB has been obtained for the frequency range (69.490-70.374) GHz, (51.896-52.119) GHz. These parameters can be analyzed in comparative analysis Figure 12(a), (b), (c).

The next structure called ANT-S4 with GS1+GS2+GS3+Reflector+Superstate1 and Superstate2 are resonating on three bands; these bands are m1=63.241GHz (61.109-66.0551) GHz, m2=41.931GHz (41.275-42.420) GHz, 76.482GHz (73.976-79.084) GHz and the RL values are -24.884dB, -14.271dB, -16.731dB respectively. And the maximum gain is 11.8715 dBi. Also, the AR<3dB are (76.8606-77.3000) GHz and (69.928-70.807) GHz. The diagrammatic representation for the ANT-S1, S2, S3, S4, and S5 are given in Figure 11 (a),(b),(c),(d),(e), and the return loss, gain and AR values are represented in Figure 9(a),(b),(c).

To analyze the antenna resonances, two antennas are compared ANT-S5'(without Patch with all methodologies implemented) and ANT-S5. The S_{11} and Gain with frequencies are shown in Figure 10 (a), (b). ANT-S5' is resonating on the three bands without patch structure, while with the patch it is resonating on four bands, so it can be analyzed that one band is from the Patch structure. The ANT-S5' resonating frequencies are m1 82.758GHz (78.690-89.452) GHz, m2=58.8621GHz (57.9406-59.6127) GHz, m3=41.4828GHz (40.653-41.979) GHz and the return loss values are -24.6887dB, -11.199dB, -16.196dB corresponds to center frequencies. Also, the gain is approximately the same in ANT-S5 and ANT-S5' shown in Figure 10 (b).

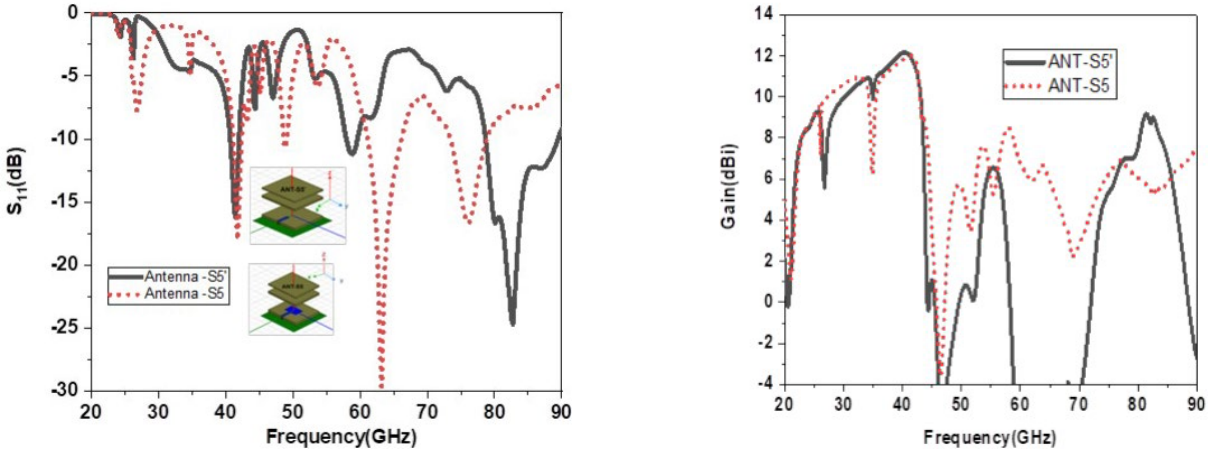

(a) (b)

Figure 10. (a) S_{11} Parameter of ANT-S5 and ANT-S5' (b) Gain Parameter of ANT-S5 and ANT-S5'

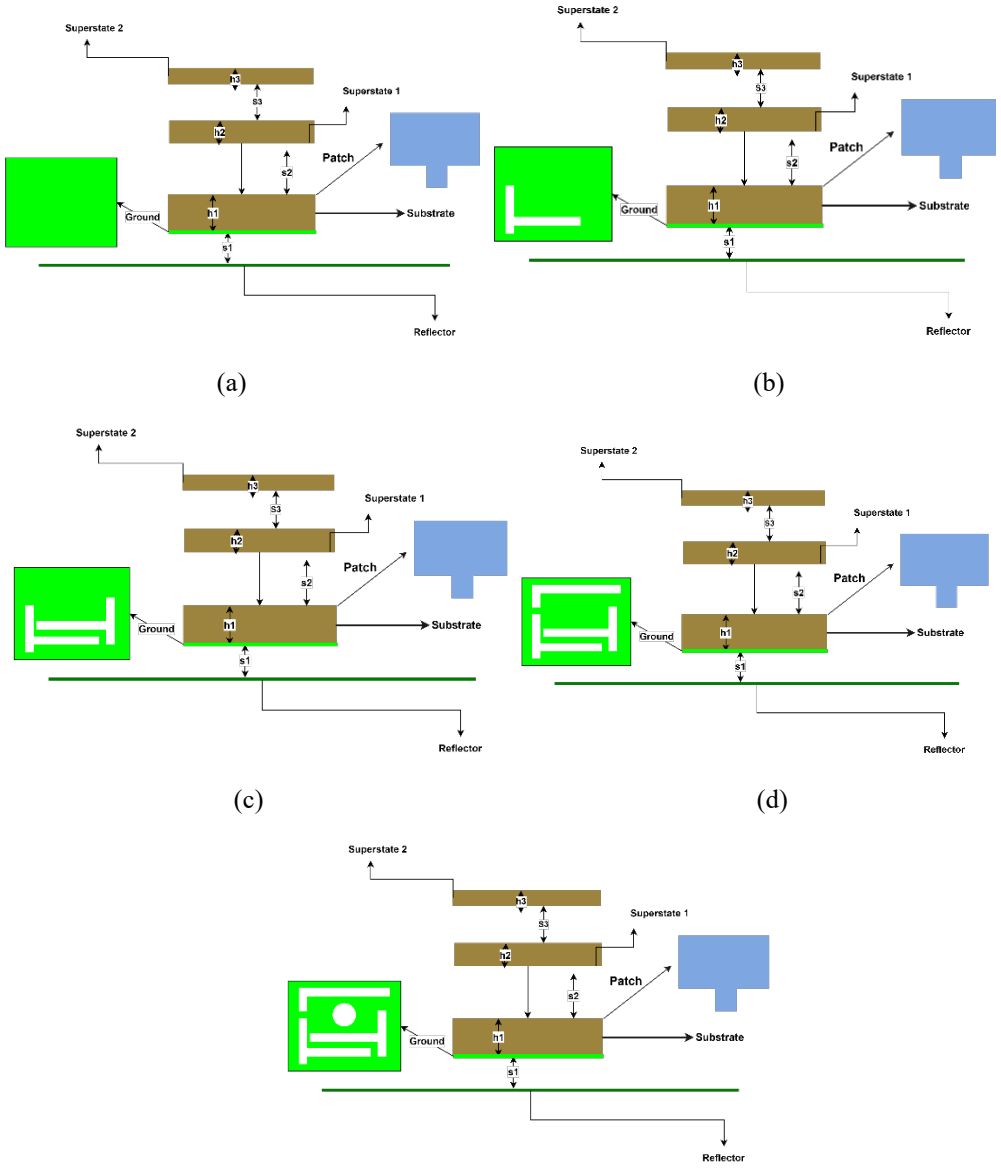

(a) (b)

(c) (d)

(e)

Figure 11. Proposed ANT Structures (a) ANT-S1 (b) ANT-S2 (c) ANT-S3 (d) ANT-S4 (e) ANT-S5

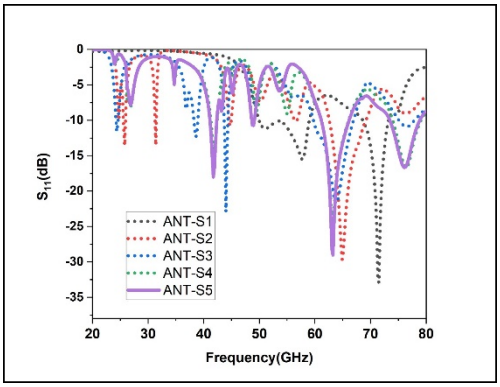

(a)

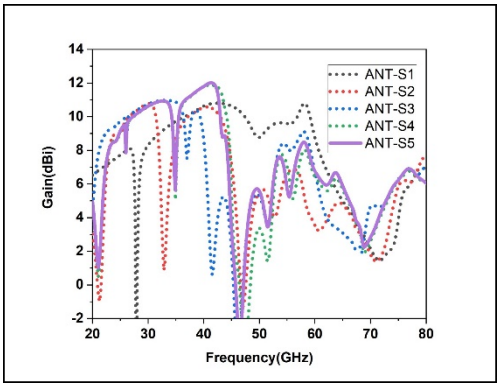

(b)

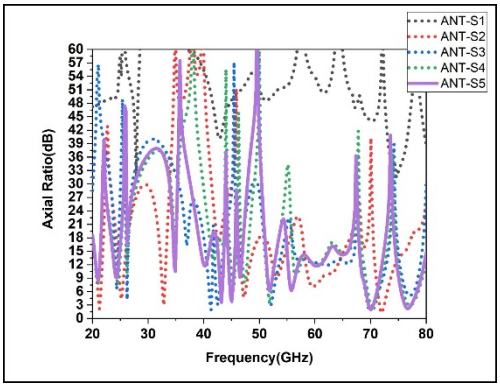

(c)

Figure 12. (a) Different ANT Comparison (a) Return Loss (b) Gain (c) Axial Ratio

ANT-S1-S5, the representation of the characteristics can be visualized from Table 4. From the table, it can be analyzed that ANT-S5 is providing the maximum gain, which is 12.02dBi as compared to ANT-S1, S2, S3, and S4. Also, from Table 4, the different ANT structures can be compared in terms of resonating bands; more resonating bands (five) are present in ANT-S2 and ANT-S3 compared to ANT-S5. Also, in ANT-2 the AR<3dB bands are three, while in the case of ANT-S5, two AR >3dB bands are present, but the gain in ANT-S2 and ANT-S3 is less as compared to ANT-S5.

Table 4. Performance parameters with different ANT

Proposed ANT	Resonating Bands (GHz)	Maximum Gain (dBi)	AR<3dB
ANT-S1	68.6162-73.260 49.949-59.005	10.82	No bands
ANT-S2	62.582-69.179 56.375-56.736 44.55-44.938 31.247-31.465 25.552-25.924	10.79	71.624-72.450 32.8271-32.8278 21.175-21.298
ANT-S3	24.219-24.596 38.235-38.944 43.683-44.351 59.712-66.937 75.074-77.898	10.975	69.490-70.374 51.896-52.119
ANT-S4	61.109-66.0551 41.275-42.420 73.976-79.084	11.87	76.860-77.3000 69.928-70.807
ANT-S5	41.110242.347 48.637-49.106 61.142-66.137 73.4655-78.859	12.021	76.1777-77.279 69.662-70.509

Also, for the ANT-S5 the vector current distribution is represented in Figure 13 (a),(b),(c),(d) for the different resonating frequencies, and the surface current path of the ground plane can be analyzed. Another performance parameter called directivity is important in the antenna design. For the proposed ANT-S5 the directivity of the antenna at the different resonating frequencies has been represented in Figure 14(a), (b), (c), (d).

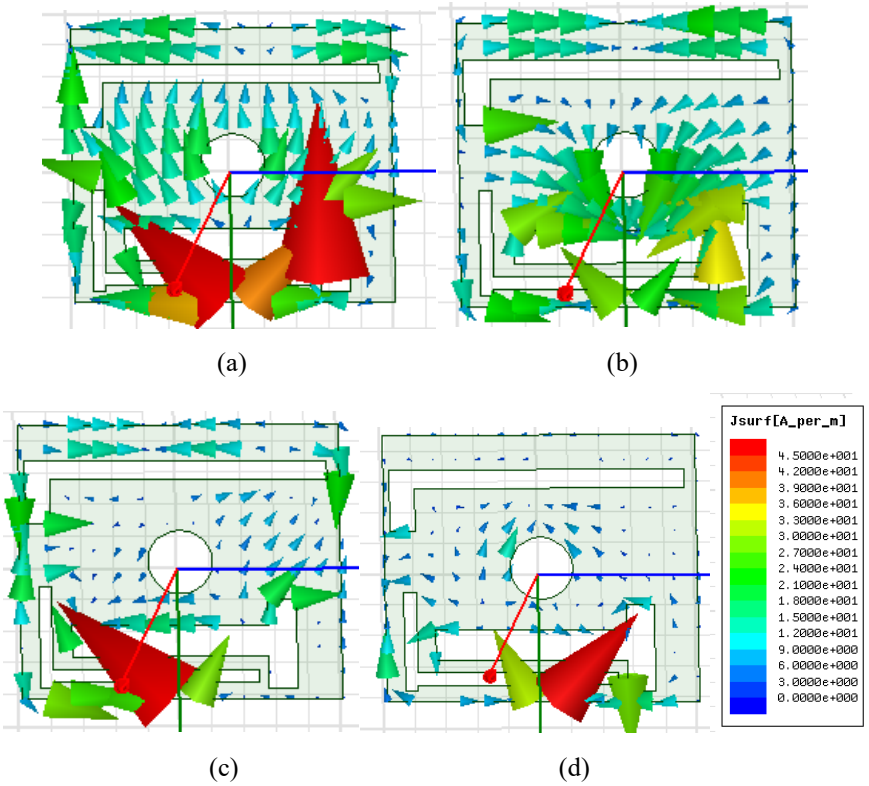

Figure 13. Proposed ANT S-5 current Distribution at (a) 41.724GHz (b) 48.9655GHz (c) 63.241GHz (d) 76.069GHz

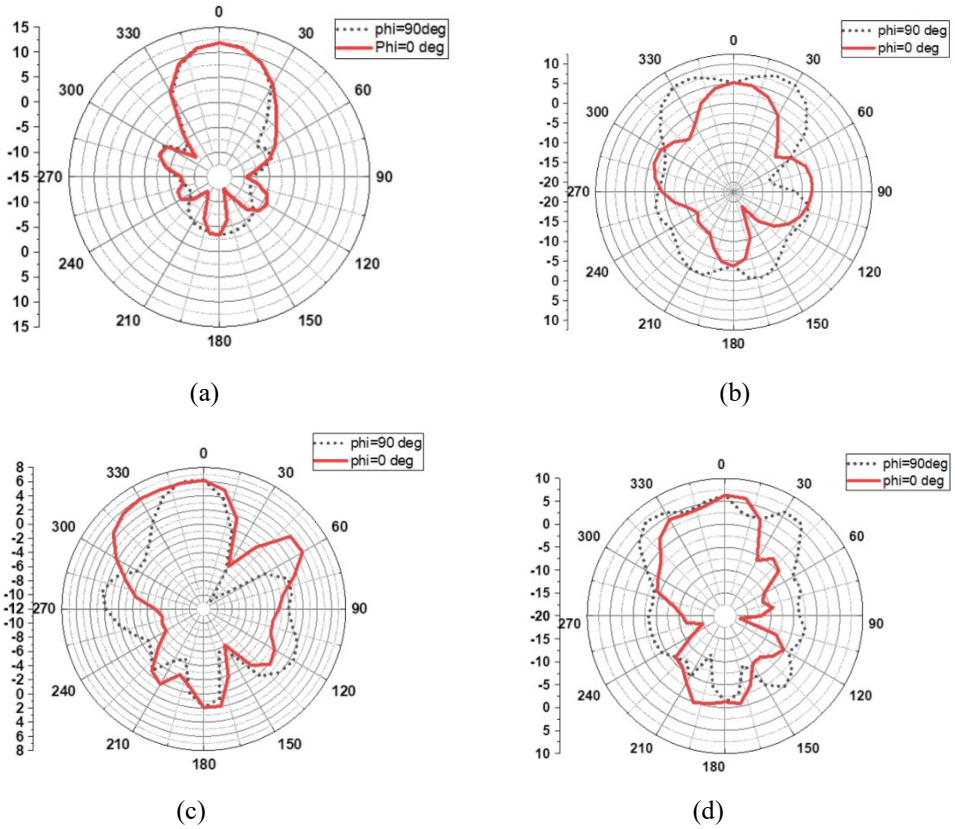

Figure 14. Directivity plot of Proposed ANT-S5 (a) 41.724GHz (b) 48.965 (c) 63.241GHz (d) 76.069GHz.

The proposed ANT structure has been compared with the previous literature which is given in Table 5. Table 5 represents that Ref [18], [19], [21] are single-band resonating, and the gain is also less as compared to a proposed structure in [19], [20], [21]. In ref. [18], the gain is almost equal, but the antenna is single-band resonating, and in the proposed structure, the antenna is quad-band resonating with a good gain.

Table 5. Proposed antenna characteristics comparison with previous literature

Ref.	Resonating Frequency	Frequency Bands	Maximum Gain/ Peak Gain(dBi)	Implementation Technique
[23]	57–64 GHz	Single	12	Metamaterial
[24]	32.5-35	Single	9.7	Substrate integrated waveguide (SIW)
[25]	700–960 MHz 1710–2690 MHz 25–30 GHz	Three	7	Vivaldi element
[26]	22-28.4	Single	10.7	Slotted
Proposed Antenna	41.7241GHz 48.9655GHz 63.2414GHz 76.069GHz	Quad	12.021	DGS +Double Superstates

4. CONCLUSION

In the proposed article, the quad-band antenna with the DGS, reflector, and double superstates has been implemented. In the ground plane, the different shape slots are etched out, and the performance characteristics have been analyzed. For performance enhancement, the reflector surface and superstates has been implemented. The given antenna structure (ANT-S5) has the bandwidth of 1.23 GHz, 0.4 GHz, 4.9 GHz, 5.3 GHz at the resonating frequencies 41.7241GHz, 48.9655GHz, 63.2414GHz, 76.069GHz respectively. The high gain achieved is 12.02dBi with the two AR<3dB bands, which are (76.1777-77.279) GHz, and (69.662-70.509) GHz. The proposed structure is simple in design with compact size features, provides good antenna gain and multiband characteristics and it is useful for 5G mm-wave applications.

REFERENCES

[1] Abutarboush HF, Li W, Shamim A. Flexible-screen-printed antenna with enhanced bandwidth by employing defected ground structure. IEEE Antennas and Wireless Propagation Letters. 2020;19(10):1803-7.

[2] Zhu S, Liu H, Wen P, Chen Z, Xu H. Vivaldi antenna array using defected ground structure for edge effect restraint and back radiation suppression. IEEE antennas and wireless propagation letters. 2019;19(1):84-8.

[3] Wang W, Wu Y, Wang W, Yang Y. Isolation enhancement in dual-band monopole antenna for 5G applications. IEEE Transactions on Circuits and Systems II: Express Briefs. 2020;68(6):1867-71.

[4] Naqvi SI, Naqvi AH, Arshad F, Riaz MA, Azam MA, Khan MS, et al. An integrated antenna system for 4G and millimeter-wave 5G future handheld devices. IEEE Access. 2019;7:116555-66.

[5] Mahmoud KR, Montaser AM. Design of compact mm-wave tunable filtenna using capacitor loaded trapezoid slots in ground plane for 5G router applications. IEEE Access. 2020;8:27715-23.

[6] Guha D, Kumar C, Pal S. Improved cross-polarization characteristics of circular microstrip antenna employing arc-shaped defected ground structure (DGS). IEEE Antennas and Wireless Propagation Letters. 2009;8:1367-9.

[7] Kumar C, Pasha MI, Guha D. Microstrip patch with nonproximal symmetric defected ground structure (DGS) for improved cross-polarization properties over principal radiation planes. IEEE Antennas and Wireless Propagation Letters. 2015;14:1412-4.

[8] Sung Y, Kim M, Kim Y. Harmonics reduction with defected ground structure for a microstrip patch antenna. IEEE Antennas and Wireless Propagation Letters. 2003;2:111-3.

[9] Kumar C, Guha D. Reduction in cross-polarized radiation of microstrip patches using geometry-independent resonant-type defected ground structure (DGS). IEEE Transactions on Antennas and Propagation. 2015;63(6):2767-72.

[10] Kumar C, Pasha MI, Guha D. Defected ground structure integrated microstrip array antenna for improved radiation properties. IEEE Antennas and Wireless Propagation Letters. 2016;16:310-2.

[11] Guha D, Biswas S, Biswas M, Siddiqui JY, Antar YM. Concentric ring-shaped defected ground structures for microstrip applications. IEEE antennas and wireless propagation letters. 2006;5:402-5.

[12] Kumar C, Guha D. Asymmetric and compact DGS configuration for circular patch with improved radiations. IEEE Antennas and Wireless Propagation Letters. 2019;19(2):355-7.

[13] Hussein AH, Abdullah HH, Attia MA, Abada AM. S-band compact microstrip full-duplex Tx/Rx patch antenna with high isolation. IEEE Antennas and Wireless Propagation Letters. 2019;18(10):2090-4.

[14] Kumar C, Guha D. Asymmetric geometry of defected ground structure for rectangular microstrip: A new approach to reduce its cross-polarized fields. IEEE Transactions on Antennas and Propagation. 2016;64(6):2503-6.

[15] Chiang KH, Tam KW. Microstrip monopole antenna with enhanced bandwidth using defected ground structure. IEEE antennas and wireless propagation letters. 2008;7:532-5.

[16] Mikulasek T, Georgiadis A, Collado A, Lacik J. 2$\,\times\, $2 Microstrip Patch Antenna Array Fed by Substrate Integrated Waveguide for Radar Applications. IEEE Antennas and Wireless Propagation Letters. 2013;12:1287-90.

[17] Wang H, Huang X, Fang D, Han G. A microstrip antenna array formed by microstrip line fed tooth-like-slot patches. IEEE Transactions on antennas and propagation. 2007;55(4):1210-4.

[18] Wang H, Huang X, Fang D. A single layer wideband U-slot microstrip patch antenna array. IEEE antennas and wireless propagation letters. 2008;7:9-12.

[19] Gray D, Lu JW, Thiel DV. Electronically steerable Yagi-Uda microstrip patch antenna array. IEEE Transactions on antennas and propagation. 1998;46(5):605-8.

[20] Chen X, Zhao F, Yan L, Zhang W. A compact filtering antenna with flat gain response within the passband. IEEE Antennas and Wireless Propagation Letters. 2013;12:857-60.

[21] Liu W, Chen ZN, Qing X. Metamaterial-based low-profile broadband aperture-coupled grid-slotted patch antenna. IEEE Transactions on antennas and propagation. 2015;63(7):3325-9.

[22] Gao G-P, Yang C, Hu B, Zhang R-F, Wang S-F. A wide-bandwidth wearable all-textile PIFA with dual resonance modes for 5 GHz WLAN applications. IEEE Transactions on Antennas and Propagation. 2019;67(6):4206-11.

[23] Dadgarpour A, Zarghooni B, Virdee BS, Denidni TA. Improvement of gain and elevation tilt angle using metamaterial loading for millimeter-wave applications. IEEE Antennas and Wireless Propagation Letters. 2015;15:418-20.

[24] Cheng YJ, Fan Y. Millimeter-wave miniaturized substrate integrated multibeam antenna. IEEE Transactions on antennas and propagation. 2011;59(12):4840-4.

[25] Kurvinen J, Kähkönen H, Lehtovuori A, Ala-Laurinaho J, Viikari V. Co-designed mm-wave and LTE handset antennas. IEEE Transactions on Antennas and Propagation. 2018;67(3):1545-53.

[26] Rodriguez-Cano R, Zhang S, Zhao K, Pedersen GF. Mm-wave beam-steerable endfire array embedded in a slotted metal-frame LTE antenna. IEEE Transactions on Antennas and Propagation. 2020;68(5):3685-94.

